Korean J. Chem. Eng., 32(4), 694-701 (2015)
DOI: 10.1007/s11814-014-0242-9

pISSN: 0256-1115
eISSN: 1975-7220

Enhanced bio-ethanol production via simultaneous saccharification and fermentation through a cell free enzyme system prepared by disintegration of waste of beer fermentation broth

Shaukat Khan, Mazhar Ul-Islam, Waleed Ahmad Khattak, Muhammad Wajid Ullah, Bowan Yu, and Joong Kon Park†

Department of Chemical Engineering, Kyungpook National University, Daegu 702-701, Korea
(*Received 27 March 2014 • accepted 21 August 2014*)

Abstract−Current study illustrates the effect of high yeast cell density contained in the waste of beer fermentation broth (WBFB) on bio-ethanol production through simultaneous saccharification and fermentation (SSF). WBFB was disintegrated (DW) and comparatively evaluated against nondisintegrated WBFB (NDW) for bio-ethanol production at variant temperatures. Final bio-ethanol levels of 36.38 g/L and 18.65 g/L at 30 °C, 4.45 g/L and 43.23 g/L at 40 °C, and 2.32 g/L and 6.83 g/L at 50 °C were achieved with 20% NDW and DW, respectively, after 12 h. DW carried out the simultaneous saccharification and fermentation (SSF) process through cell free enzyme system and was capable of bio-ethanol production beyond the microbial growth temperature (>30 °C) of NDW system. The increase in sediment concentration in DW positively influenced the production capabilities of the system producing 43.23 g/L, 54.39 g/L and 62.82 g/L bio-ethanol with 20, 30 and 40% sediments at 40 °C, respectively. The retardation of bioethanol production at elevated temperature (50 °C) was expected to be caused by denaturing or digesting of certain enzymes as observed through SDS-PAGE. FTIR analysis also showed the appearance of a new band at approximately 1,590 cm^{-1} due to unfolding of polypeptide chains at 50 °C. The overall study reveals the positive influence of increased cell density on ethanol production and presents evidence for decreased fermentation beyond certain temperature limits.

Keywords: Bio-ethanol, Disintegration, Cell-free Enzyme System, Saccharification, Glycolytic, Fermentation

INTRODUCTION

The production of bio-ethanol from alternative sources such as industrial and agricultural waste and non-edible materials has increasingly attracted attention in recent years. Bio-ethanol provides an alternative renewable energy source for rapidly depleting non-renewable fossil fuel reservoirs. In addition to their high cost, fossil fuels lead to serious environmental issues [1]. A great deal of attention has been focused on discovering inexpensive renewable energy sources and developing new production techniques. Food and fuel competition issues have been resolved by shifting towards non-edible raw sources, such as fermentation of bagasse [2], sugarcane leaves [3], tree sawdust [4], and food and agricultural wastes [1,5,6]. The production of bio-fuels from these raw materials will not only sideline the use of edible items for the stated purpose but will also lead to the resolution of serious environmental issues. Currently, the initial pretreatment and capital cost of these biomass materials are a major economic concern [7].

In addition to the pretreatment and capital cost issues, conventional microbial fermentation processes are adversely affected by substrate and product concentrations. Recent advancements in simultaneous saccharification and fermentation (SSF) have greatly reduced the inhibition effect [1]. However, the difference in the temperature optima of saccharification and fermentation processes is a major barrier in the development of an effective SSF process [8]. To solve this problem, genetically modified microbial thermotolerant strains were developed that exhibit high fermentation activities at elevated temperatures [9]. This strategy was successful in producing bio-ethanol but could not resolve the major barrier (optimal temperature differences) associated with the process. Therefore, a more advanced approach was employed for the fermentation process via complete cell assembly without living cells [10,11]. This cell-free enzyme system overcomes the limitation of ethanol and/or glucose inhibition, prevents the accumulation of aberrant intermediate metabolites [10], and controls for variables such as cofactor concentration, pH, and ionic strength [11]. A number of studies have reported successful bio-ethanol production from pure glucose using a cell-free enzyme system [10,11]. Welch and Scopes [10] described a reconstituted cell-free system consisting of a series of 12 purified enzymes (from yeast, rabbit muscle) and cofactors (Sigma Chemical Co.) and evaluated it for bio-ethanol production utilizing 18% glucose [10]. The system successfully carried out glycolysis and fermentation with a 50% yield of bio-ethanol. Although the approach was successful, the expensive purified enzymes and cofactors prevented its industrial scale up. Moreover, the fermentation was at 30 °C, which is within the optimum fermentation temperature range of yeast. Khattak et al. developed a cell-free enzyme system from pure yeast cell culture [12]. The presence of the glycolytic and fermentation enzymes and cofactors involved in the fermentation process was identified and the system was evaluated for bio-ethanol production at elevated temperatures using pure glucose as the substrate. The system was more effective at 40 °C, which might help

†To whom correspondence should be addressed.
E-mail: parkjk@knu.ac.kr

in resolving the temperature barrier of SSF [12].

Waste of beer fermentation broth (WBFB) has been extensively evaluated for bio-ethanol production [8,13,14]. Successful bio-ethanol production was achieved from bare WBFB without additional enzymes, carbon sources, or microbial cells [13]. Proteomic analysis of WBFB showed the presence of hydrolyzing enzymes including cell wall-, saccharide-, lipid-, polyphenol-, and thiol-hydrolyzing enzymes [15], protein degrading enzymes, and yeast glycolytic and fermentation enzymes [8]. The existence of hydrolyzing, glycolytic, and fermentation enzymes as well as live yeast cells in WBFB provided insight for carrying out SSF process. Accordingly, SSF was performed using original WBFB without the addition of any carbon source, and a significant increase in bio-ethanol production was observed with the addition of only 3% sediments at 67 °C during the process [8]. In that study, malt hydrolyzing enzymes were used as saccharification source, while viable yeast cells and the cellular materials extruded out from thermally ruptured yeast cells were speculated to conduct fermentation.

To ensure the involvement of cell free machinery in the fermentation process, we developed a pure cell-free enzyme system based on single yeast cell line [12]. The system was successful in bioethanol production without live yeast cells using glucose as carbon source. However, besides being capable of bioethanol production, the reported cell-free system offered some limitation. The development of large scaled yeast cultures and their disintegration is itself a difficult and time consuming process. Also, the external supply of carbon source increases the capital cost of the bio-ethanol production. The use of cheaper raw sources for development of such systems can significantly enhance the economic feasibility of the process. WBFB contains a high density of viable yeast cells and is also rich in essential carbon sources required for bio-ethanol production [14]. Therefore, we investigated the yeast cells in WBFB as the source of cell free enzymes and carried out bio-ethanol production without the addition of an external carbon source. Towards this aim, we disintegrated WBFB to develop the cell free enzyme system containing the glycolytic and fermentation enzymes from lysed yeast cells as well as the saccharification enzymes from malt contained in the WBFB. The DW was compared for its SSF capabilities against the NDW, containing saccharification enzymes from malt and live yeast cells, at various temperatures. We investigated the effect of high sediments concentration on bio-ethanol production and the reasons for process retardation beyond specific temperature range.

MATERIALS AND METHODS

1. Storage of WBFB and Separation of Sediments from WBFB

WBFB was obtained from the Ariana Hotel beer industry in Daegu, Korea and was stocked as reported previously [13]. WBFB solid sediments were separated from the supernatant by centrifugation at 3,500 rpm for 20 min.

2. Development of Disintegrated WBFB (DW)

Original WBFB containing 20% sediments and 80% supernatant was disintegrated to develop the DW system using three different methods: ultrasonication, heat treatment, and bead beating. For ultrasonication, freshly obtained WBFB (10 mL) were added to sterilized glass vials. The amplitude and power of the ultrasonicator (Ningbo Sklon, SKL-IIDN, China) were adjusted to 50 kHz and 100 W, respectively. Sonication was performed with 10 sec pulse on and 5 second pulse off. Sample vials were kept in an ice bath during cell disruption to prevent overheating. Samples were collected after 15, 30, 45, and 60 min of sonication. For heat treatment, vials were incubated at 67 °C with agitation (150 rpm) and collected after 15, 30, 45, and 60 min. In the bead beating method, equal volumes of WBFB and chilled glass beads (1,000-μm; Daihan Scientific SI4504) were placed in a sterilized glass vial and vortexed for 15, 30, 45, and 60 min. Samples were chilled in ice at regular intervals of 3 min to avoid thermal denaturation of the proteinaceous cellular matrix [12].

The samples obtained from ultrasonication, heat treatment, and bead beating were analyzed for cell morphology and cell density using the colony forming unit method (CFU) and total protein concentrations through Bradford assay. LC-MS/MS Q-TOF analysis was performed to identify yeast glycolytic and fermentation enzymes and malt hydrolyzing enzymes in the DW. Samples were prepared and characterized following the procedures described previously [8]. The cell-free lysate was collected with a sterile syringe and evaluated for bio-ethanol production without further processing.

3. Parametric Analysis of DS for Enhanced Bio-ethanol Production

The effect of temperature and sediments concentration on maximum bio-ethanol production using NDW and DW was determined. Both the systems were incubated at 30, 40, and 50 °C with agitation (150 rpm) for 12 h. Samples were collected and analyzed for bio-ethanol production. To determine the effect of high sediments concentration in DW, equal volume of WBFB supernatant was taken in different vials and 20%, 30% and 40% (based on the total volume of WBFB) sediments were added externally, followed by disintegration to develop the disintegrated systems DW20, DW30 and DW40, respectively. The DW20, DW30 and DW40 were incubated in 5 mL glass vials at 40 °C with agitation (150 rpm) for 12 h for bio-ethanol production. During incubation, samples were collected and analyzed for bio-ethanol production and glucose and starch consumption.

4. Analytical Procedures

Before and after disintegration, the protein concentration was determined via Bradford assay using bovine serum albumin as a standard [8]. The concentration of glucose and starch in the fermentation broth was determined by a glucose assay kit (Sigma GAGO-20) and starch assay kit (Sigma SA-20), respectively. The amount of bio-ethanol produced was measured with a UV-visible spectrophotometer (Sunil Eyela Co., Ltd., China) and an ethanol assay kit (Bio Assay Systems, Hayward, CA, USA). The absorbance was measured at 580 nm. Removal of glucose from the fermentation broth was performed before bio-ethanol quantification by using a saccharide removal kit (Bio Assay Systems, Hayward, CA, USA). The bio-ethanol yield was calculated from the following formula:

$$\text{Percent yield} = \frac{\text{Actual yield}}{\text{Theoretical yield}} \times 100$$

An ATP assay kit (ab83355; Abcam, England) and NAD^+/NADH assay kit (ab65348; Abcam, England) were used to determine the concentrations of ATP and NAD^+ in the NDW and DW system

[12]. All experiments were performed in triplicate and differences between means were considered significant at $p \leq 0.05$. Means and standard deviation of the results were calculated with Microsoft Excel® software (Redmond, WA, USA).

5. Characterization of DW and Enzyme System

5-1. Evaluation of Enzyme Integrity in DW through Protein Analysis

Original WBFB, initially obtained DW and after incubation at 30, 40 and 50 °C for 12 h were investigated for the presence of malt hydrolyzing and yeast glycolytic and fermentation enzymes by 15% polyacrylamide gradient SDS-PAGE under reducing conditions in a Bio-Rad mini-gel apparatus [8,15]. A protein ladder with a range of 10-170 kDa (Page Ruler™; Thermo Scientific, Waltham, MA, USA) was used as a standard and protein bands were visualized by Coomassie Brilliant Blue R-250 staining (Sigma, UK).

5-2. Field Emission Scanning Electron Microscope (FE-SEM) Analysis

FE-SEM images of freeze-dried original WBFB, initially obtained DW and after incubation at 30, 40 and 50 °C for 12 h were recorded on a Hitachi S-4800 and EDX-350 (Horiba) FE-SEM (Tokyo, Japan). Briefly, samples were fixed onto a brass holder and then coated with osmium tetra oxide (OsO_4) by using a VD HPC-ISW osmium coater (Tokyo Japan) prior to FE-SEM observation.

5-3. Fourier Transform Infrared (FTIR) Spectroscopy

FTIR of freeze-dried original WBFB, initially obtained DW and after incubation at 30, 40 and 50 °C for 12 h were recorded with a PerkinElmer FTIR spectrophotometer [spectral range: 4,000-400 cm^{-1}; beam splitter: Ge coated on KBr; detector: DTGS; resolution: 0.25 cm^{-1} (step selectable); Spectrum GX & Autoimage, USA]. For analysis, the samples were mixed with KBr pellets (IR grade; Merck, Germany) and further processed to obtain IR data.

RESULTS AND DISCUSSION

1. Disintegration of WBFB and Development of Cell-free Enzyme System

Numerous approaches have been reported for extracting cellular proteins [16-19], including bead beating, ultrasonication, and heat treatment, which were comparatively evaluated in this study for the disintegration of WBFB containing yeast cells. The increased protein concentration and corresponding decrease in cell density associated with increased treatment time are shown in Table 1. Cellular morphology was analyzed microscopically during disintegration (Fig. 1S). Heat treatment at 67 °C resulted in a small increase in protein concentration, whereas cell viability was completely lost within 30 min of incubation due to thermal stress [8]. The small increase in protein concentration was supported by the negligible cell lysis observed microscopically (Fig. 1S). Ultrasonication resulted in significantly increased protein concentration with a corresponding decrease in cell density (Table 1), and microscopic images also indicated the complete rupture of yeast cells after 1 h of ultrasonication (Fig. 1S). From the results (Table 1 and Fig. 1S), bead beating was the most reliable for extraction of cellular proteins from yeast cells in WBFB sediment among the three techniques evaluated. The initial CFU of the yeast culture in WBFB was 2.1×10^9 CFU/mL, which decreased with increasing bead beating time (Table 1). After 45 min of bead beating, cell viability was almost completely lost and the protein concentration increased from 2.64 to 16.25 g/L. The increase in protein concentration, decrease in cell viability, and cell rupture as seen by microscopic imaging are all in agreement (Table 1 and Fig. 1S), and indicate bead beating to be the most suitable method for obtaining cell-free lysate.

Table 1. WBFB was disintegrated using the bead beating, ultrasonication and heat treatment methods. Treatment time (min), increase in protein concentration (mg/mL), and corresponding decrease in cell density (CFU/mL) are listed

Disintegration method	Treatment time (min)	Protein conc. (mg/mL)	Cell density (CFU/mL)
----	0	2.64±0.043	2.1×10^9
Bead beating	15	12.91±0.06	2.3×10^6
(bead size	30	15.69±0.05	6.8×10^3
~1,000 μm)	45	16.13±0.05	3.8×10^2
	60	16.25±0.04	1.7×10^1
Ultrasonication	15	11.17±0.05	3.1×10^6
	30	13.97±0.05	7.6×10^3
	45	14.32±0.04	5.3×10^2
	60	14.49±0.04	3.7×10^1
Heat treatment	15	2.83±0.05	7.5×10^5
(67 °C)	30	3.39±0.05	0
	45	3.56±0.04	0
	60	3.78±0.03	0

LC-MS/MS Q-TOF analysis of disintegrated WBFB sediments was performed to identify the glycolytic and fermentation enzymes from yeast in the DW. The yeast cellular enzymes categorized as glycolytic, fermentation and protease enzymes [20] are listed in Table 1S. These enzymes are probably involved in the fermentation activity at elevated temperatures without viable yeast cells. The activity of certain protein-hydrolyzing enzymes (carboxypeptidase yscY and aminopeptidase yscII), identified in the cell lysate, can damage the cell-free enzyme system in the DS by disrupting peptide bonds [21].

Cofactors including ATP and NAD^+ are necessary for the cell-free fermentation process. These cofactors are required not only for initiation but also for the non-stop propagation of the process [22]. The presence of these cofactors in WBFB supernatant has been reported previously [12]. Quantitative evaluation of the NDW revealed concentrations of ATP and NAD^+ as 3.27 mM and 2.73 mM, which increased to 3.51 mM and 2.94 mM in the DW20, 3.76 mM and 3.09 mM in the DW30 and 3.95 mM and 3.29 mM in the DW40, respectively. Viable yeast cells in NDW contain these cofactors and can efficiently carry out the glycolytic and fermentation processes. However, the disintegrated systems (DW20, DW30 and DW40) containing yeast cell free enzymes require a sufficient amount of these cofactors to ensure the feasibility of the fermentation process. During disintegration of the yeast cells the cellular matrix containing cofactors is released to the surrounding media, which results in an increase in their concentration [12]. The observed concentration of cofactors is sufficient for the initiation of a cell-free fermentation process [23,24]. Therefore, no additional cofactors were added exogenously to the systems.

2. Effect of Temperature on Bio-ethanol Production Using DW and NDW

The current study was conducted to determine the effect of higher yeast cell density contained in WBFB sediments on bio-ethanol production at elevated temperatures. Furthermore, the optimal conditions for maximal bio-ethanol production using disintegrated WBFB was determined. NDW and DW were comparatively evaluated for bio-ethanol production at various temperatures (30, 40, and 50 °C). The bio-ethanol produced during 12 h of incubation by NDW and DW is shown in Fig. 1(a). Bio-ethanol was produced at all three temperatures with a maximum production of 36.38 g/L and 18.65 g/L at 30 °C, 4.45 g/L and 43.23 g/L at 40 °C, and 2.32 g/L and 6.83 g/L at 50 °C with NDW and DW, respectively, after 12 h. NDW-containing live cells were active at 30 °C (optimum growth temperature: 30-32 °C); therefore, they showed maximum bio-ethanol production at 30 °C. However, at elevated temperatures (40 °C and above) cells lost their fermentation activity due to thermal shock. Contrary, DW could effectively withstand elevated temperatures and showed maximum activity at 40 °C. The different production capabilities beyond optimal cell growth temperatures illustrated the contribution of exogenous enzymes to bio-ethanol production. Enzyme activity increases with increased temperature up to a certain limit. Shuler and Kargi reported a 1.8-fold increase in enzyme activity with an increase in temperature from 30 °C to 40 °C [25]. Additionally, a comparative analysis of yeast cell-free enzyme system activities at 30 °C and 38 °C showed improved results at 38 °C [26]. These results indicate that cell-free enzymes in DW were active at a higher temperature compared to the whole yeast cells, and effectively carried out fermentation. This could be a reason why DW demonstrated bio-ethanol production at elevated temperatures without live cells. However, thermal denaturation of enzymatic proteins causes alteration of the active sites and thus inhibits substrate binding to the enzyme [12,27]. Therefore, a decrease in bio-ethanol production is observed when the fermentation is at 50 °C. Moreover, the approach of using DW for bio-ethanol production justifies their application on industrial scale bio-ethanol production from simple sugar at elevated temperatures.

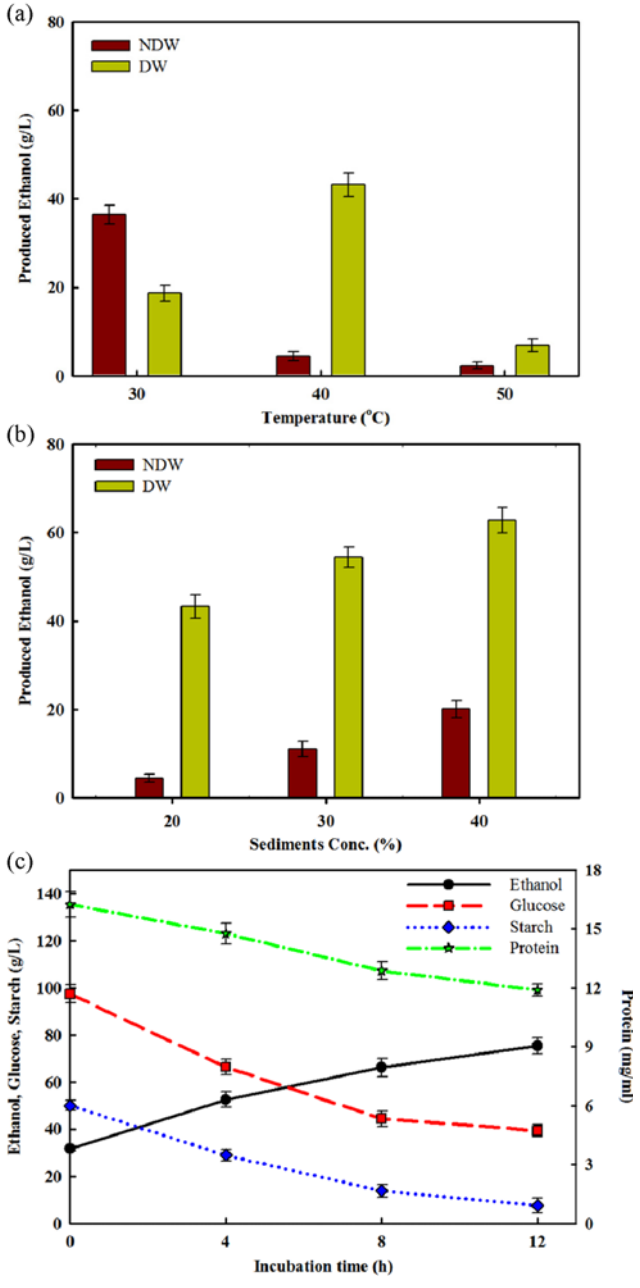

Fig. 1. Parametric analysis of DW for high bio-ethanol production. (a) Effect of temperature on bio-ethanol production through fermentation by NDW and DW. Experiments were conducted at 30, 40, and 50 °C for 12 h and 150 rpm. (b) Effect of increased sediments concentration on bio-ethanol production using NDW and DW systems. Experiments were conducted using 20, 30 and 40% (DW and NDW) at 40 °C and 150 rpm for 12 h. (c) Starch, glucose, ethanol and protein profile for DW20 system during incubation at 40 °C and 150 rpm for 12 h.

3. Effect of Sediment Concentration on Bio-ethanol Production

The effect of increased sediments concentration on the production and yield of bio-ethanol was evaluated (Fig. 1(b)). Overall bio-ethanol production was 43.23 g/L, 54.39 g/L, and 62.82 g/L by DW20, DW30, and DW40, respectively, at 40 °C and 150 rpm after 12 h of incubation. Table 2 shows the increase in bio-ethanol production with increase in sediment concentration. According to previous studies, the enzyme concentration is directly correlated to the final product when the substrate is present in sufficient amounts [28]. It is evident from Table 2 that the highest bio-ethanol production was recorded with DW40 (62.82 g/L). Fig. 1(c) shows the profile obtained for starch, glucose, ethanol and protein concentrations for DW20 during the 12 h incubation period at 40 °C. The decrease in starch and glucose and increase in ethanol concentration is evident, while a negligible decrease in protein concentration is recorded during incubation. Table 2 shows that SSF occurs in the DW systems by the activity of saccharification enzymes from malt present in WBFB supernatant and yeast glycolytic and fermentation enzymes obtained through disintegration of yeast cells.

The saccharification enzymes from malt and the carbon sources such as soluble starch and glucose are present in the WBFB supernatant while the sediments contain a high yeast cell density [12]. DW20, DW30 and DW40 contain the same amount of saccharification enzymes, starch and glucose due to equal volume of super-

Table 2. SSF process carried out using DW20, DW30 and DW40 at 40 °C for 12 h and 150 rpm. Starch, glucose and ethanol concentrations were determined before incubation (initial values) and after incubation (final values). All experiments were performed in triplicate and average values reported with mean deviations around ±5%

Sediment conc. (%)	Starch conc. (g/L)		Starch consumed (g/L)	Glucose conc. (g/L)		Ethanol conc. (g/L)		Ethanol produced (g/L)
	Initial	Final		Initial	Final	Initial	Final	
20	50.1	7.27	42.83	97.4	41.64	31.8	75.03	43.23
30	50.1	6.87	43.23	97.4	22.28	31.8	86.19	54.39
40	50.1	6.46	43.64	97.4	7.61	31.8	94.62	62.82

natant added. However, the quantity of yeast glycolytic and fermentation enzymes will increase due to increase in sediment concentration in these systems. Thus, higher sediment concentrations are expected to enhance the rate of the fermentation process. Table 2 indicates that almost equal quantities of starch have been consumed in all three systems during 12 h of SSF. This supports the fact that saccharifying enzymes and starch both are exclusively contained in the WBFB supernatant. Additionally, it can be seen that the saccharifying activities were very high and around 80-85% starch was hydrolyzed only in 12h of incubation. The increase in sediment concentration, on the other hand, resulted in high amount of yeast glycolytic and fermentation enzymes which utilized more glucose and resulted in enhanced bio-ethanol production (Table 2). This implies that with the increase in sediment concentration the bio-ethanol production also increases. Table 2 indicates that glucose was almost completely consumed by the DW40 in 12 h of incubation, which ultimately offers the best system to be operated for effective SSF operation.

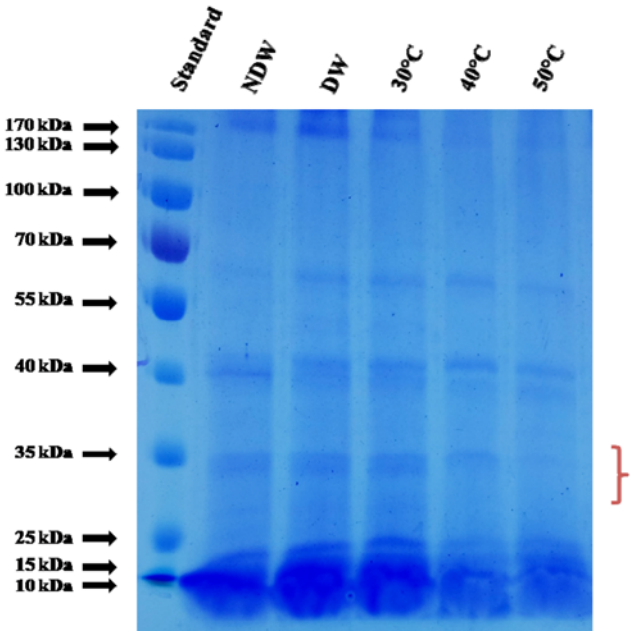

Fig. 2. SDS-PAGE shows the protein bands for original WBFB, initially obtained DW and after incubation at 30, 40 and 50 °C for 12 h are indicated. No loss of protein bands was observed after incubation at 30 and 40 °C. However, some protein bands in the range of 25-35 kDa were lost after incubation at 50 °C as indicated by a curly bracket.

4. Identification of Enzymes and Evaluation of their Thermal Stability after Incubation at Different Temperatures

SDS-PAGE analysis was performed to confirm the presence of saccharification enzymes from malt in WBFB and the existence of glycolytic and fermentation enzymes from yeast cells after disintegration (Fig. 2). It is evident from Fig. 2 that the number and intensity of bands increased in DW compared to NDW system, which confirms the release of yeast cell proteins and increase in their concentration after disintegration. The presence of both saccharification enzymes from malt and yeast glycolytic and fermentation enzymes in WBFB supernatant has been previously reported by our group [8]. The thermal stability of the cell-free enzymes in the DW system incubated at different temperatures was investigated to determine the effectiveness of the system at elevated temperatures. To accomplish this, fermentation was carried out at 30, 40, and 50 °C for 12 h using DW. Fig. 2 and Table 1S represent the SDS-PAGE analysis results of DW determined before and after incubation at 30, 40, and 50 °C for 12 h. Almost all proteins present in the initially disintegrated samples were found in the samples incubated at 30 and 40 °C. Incubation at 50 °C resulted in loss of some protein bands. However, thermal denaturation does not involve breakage of peptide bonds, and thus the loss of protein bands may be due

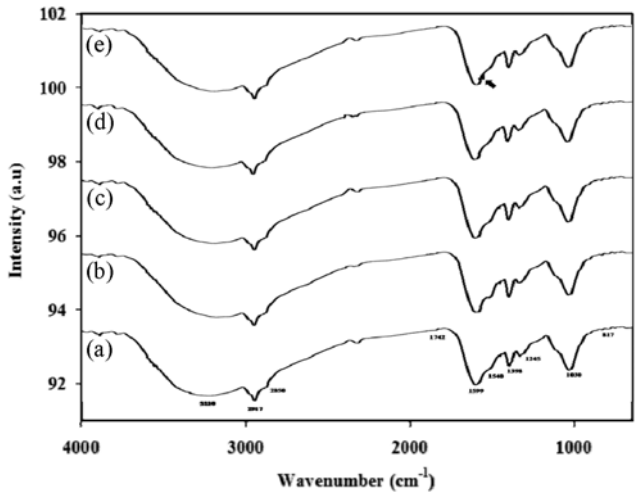

Fig. 3. Fourier transform infrared spectra of original WBFB (a), initially obtained DW (b) and after incubation at 30 °C (c), 40 °C (d) and 50 °C (e) are indicated. All characteristic peaks are indicated by their wave numbers while the peak at approximately 1,590 cm^{-1} due to thermal denaturation of proteins after incubation at 50 °C is indicated by an arrow.

to other mechanisms, such as protease enzymes observed in the yeast cells. WBFB contains a high yeast cell density mainly comprised of *S. cerevisiae* [13]. Yeast cellular proteins, extracted by disintegration, include glycolytic, fermentation, and protein digesting enzymes [20] such as carboxypeptidase yscY and aminopeptidase yscII (Table 1S). The main function of these two enzymes is the breakage of peptide bonds [21] and both aminopeptidase and carboxypeptidase show maximum activity at a temperature of approximately 50 °C and a pH of 7.0 [29-31]. Therefore, fermentation under these conditions resulted in a completely different profile indicating complete loss of some protein bands, while the same loss was not observed for samples incubated at 30 and 40 °C (Fig. 2). These results not only explain the lower bio-ethanol production at 50 °C but also emphasize the need for system purification for high-scale bio-ethanol production at elevated temperatures.

5. Structural Analysis of DW Incubated at Various Temperatures

FTIR analyses of original WBFB and DW were conducted to investigate possible compounds and also to monitor any structural changes in DW during incubation at various temperatures. FTIR spectral results are shown in Fig. 3. The IR spectrum of original WBFB and DW showed all characteristic protein peaks, with weak peaks at approximately 900-800 cm^{-1} representing modes of skeletal stretching vibrations depending on the side chain. The peak at 1,030 cm^{-1} is due to bending vibration of the NH_2 functional group. Peaks at approximately 1,245 cm^{-1} and 1,398 cm^{-1} represent C-N stretching vibration of secondary amide III bands and N-H bending vibrations of primary amide III bands, respectively. The peak at approximately 1,599 cm^{-1} is a characteristic α-helix peak. This

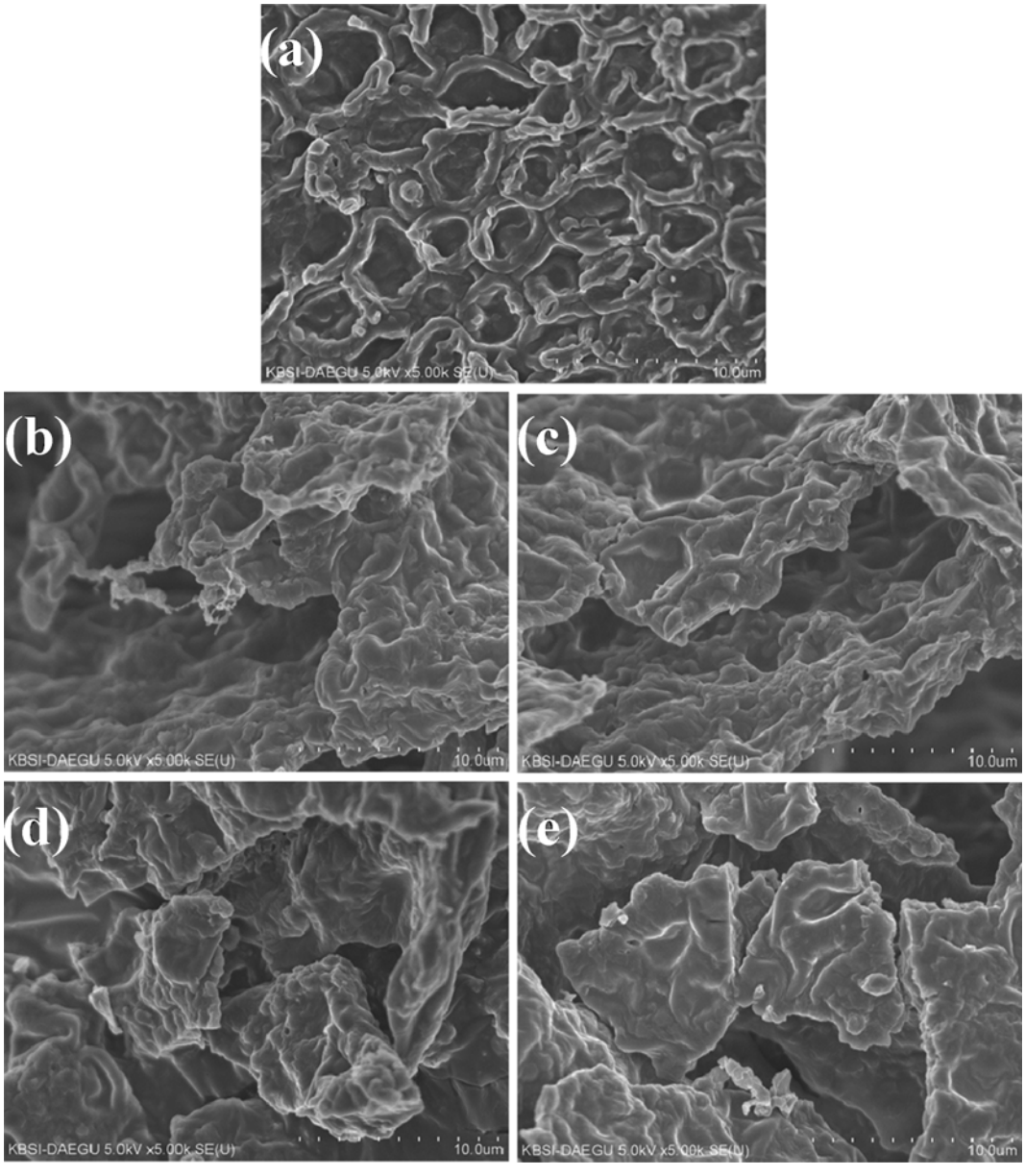

Fig. 4. Field emission scanning electron micrographs obtained for freeze-dried original WBFB (a), initially obtained DW (b) and after incubation at 30 °C (c), 40 °C (d) and 50 °C (e).

strong absorption peak is caused by the symmetric stretching vibration of C=O and N-H bonds [32-34]. Although SDS-PAGE analysis indicated loss of protein bands when the sample was incubated at 50 °C, some protein bands remained. The FTIR spectrum of this sample provided evidence for thermal denaturation of the remaining proteins. As indicated by a black arrow in Fig. 3, a weak shoulder of the main α-helix band appeared at approximately 1,590 cm^{-1} due to thermal denaturation. The frequency of this band is close to the β-sheet structure; however, it is lower than the β-sheet structure of native proteins, attributed to aggregated β-sheet structures. When polypeptide chains unfold due to thermal denaturation, they form strong hydrogen-bonded aggregated structures that give rise to distinct bands in the region 1,590-1,600 cm^{-1}, and these bands are used for monitoring thermal unfolding of proteins [35]. The peaks at approximately 2,917 cm^{-1} and 2,850 cm^{-1} are caused by CH_2 asymmetric and symmetric stretching, respectively. Finally, the broad peak at approximately 3,229 cm^{-1} represents N-H stretching in amide B and amide A linkages [36-39]. All basic protein peaks were observed in all samples, which indicates that complete denaturation does not occur after incubation at a high temperature (50 °C). The FTIR analysis results strongly support the SDS-PAGE analysis shown in Fig. 2.

Although the peak positions in the FTIR spectra indicate the presence of proteins, WBFB also contain a residual amount of carbohydrates. Most absorption peaks corresponding to the functional groups in carbohydrates overlap with those of proteins. For example, characteristic absorption bands for O-H stretching (3,000-3,500 cm^{-1}), C-H stretching (2,800-3,000 cm^{-1}), and C=O stretching (1,600-1,800 cm^{-1}) of carbohydrates coincide with protein bands [40-42]. Additionally, O-H and C-H deformation (1,200-1,400 cm^{-1}) and C-C and C-O stretching (1,000, 1,200 cm^{-1}) coincide with those of proteins. Therefore, it is clear that in the presence of both proteins and carbohydrates, the main peaks overlap and an intermixed spectrum is produced [8].

The FE-SEM images in Fig. 4 show some variation between original WBFB, initially obtained DW and after incubation at 30, 40 and 50 °C. The freeze-dried samples show flake-like shapes of sediments with varied size. It is clear that the particles in the non-incubated sample are ordered and lacking aggregation and interspaces. However, after incubation at different temperatures and agitation at 150 rpm, the smooth surface is diminished and particles aggregated, resulting in increased surface area and pores. The aggregations (coagulant) formed at elevated temperatures are reported to be the thermally denatured enzymes found in the DW [8], as prolonged exposure of enzymatic proteins to thermal stress results in unfolding of polypeptide chains and alteration of active sites. In the absence of an efficient protective system such as heat shock proteins (HSPs), unfolded polypeptides aggregate and descend in the fermentation broth [43]. The aggregation and surface pores increased as the incubation temperature increased from 30 to 50 °C (Fig. 4).

It was previously reported that beer industry sediment is produced from precipitation of live and dead yeast cells, tartrates, proteins, polysaccharides, and other insoluble materials [44]. Hydrolyzing enzymes originating from malt in WBFB are denatured and coagulate due to thermal shock during ethanol production. However, the WBFB sediments contain various other components such as carbohydrates and yeast cells. The chemical compositions of non-incubated and incubated sediments are similar, though strong heating may cause denaturation and degradation of certain enzymes and the destruction of live yeast cells.

CONCLUSIONS

The current study illustrates bio-ethanol production at elevated temperatures through SSF using high yeast cell density contained in WBFB. The malt saccharification enzymes in WBFB supernatant and the glycolytic and fermentation enzymes obtained through disintegration of viable yeast cells carried out SSF process successfully. High cell density positively influenced the bio-ethanol production. However, the yeast cell-free enzyme system obtained by disintegrating WBFB contained protein-digesting enzymes that caused the breakdown of fermentation enzymes at higher temperatures and consequently retarded bio-ethanol production.

ACKNOWLEDGEMENT

This research was supported by the Basic Science Research Program through the National Research Foundation (NRF) of Korea funded by the Ministry of Education, Science, and Technology (No. 2011-0016965) and also supported by the BK21 plus (2014-2019) Korea, (21A.2013-1800001).

REFERENCES

1. J. Prasetyo and E. Y. Park, *Korean J. Chem. Eng.*, **30**, 253 (2013).
2. C. Martin, M. Galbe, C. F. Wahlbom, B.-H. Hagerdal and L. J. Jonsson, *Enzyme Microb. Technol.*, **31**, 274 (2002).
3. S. H. Krishna, K. Prasanthi, G. V. Chowdary and C. Ayyanna, *Process Biochem.*, **33**, 825 (1998).
4. A. O. Ayeni, J. A. Omoleye, S. Mudliar, F. K. Hymore and R. A. Pandey, *Korean J. Chem. Eng.*, **31**, 1180 (2014).
5. J. Prasetyo and E. Y. Park, *Korean J. Chem. Eng.*, **30**, 253 (2013).
6. M. He, H. Qin, X. Yin, Z. Ruan, F. Tan, B Wu, Z. Shui, L. Dai and Q Hu, *Korean J. Chem. Eng.*, (2014). DOI: 10.1007/s11814-014-0108-1.
7. R. Ravikumar, B. V. Ranganathan, K. N. Chathoth and S. Gobikrishnan, *Korean J. Chem. Eng.*, **30**, 1051 (2013).
8. W. A. Khattak, T. Khan, J. H. Ha, M. Ul-Islam, M. K. Kang and J. K. Park, *Enzyme Microb. Technol.*, **53**, 322 (2013).
9. W. Y. H. Nancy, Z. Chen, A. P. Brainard and M. Sedlak, *Adv. Biochem. Eng./Biotechnol.*, **64**, 163 (1999).
10. P. Welch and R. K. Scopes, *J. Biotechnol.*, **2**, 257 (1985).
11. R. K. Scopes, *Biochem. J.*, **161**, 265 (1977).
12. W. A. Khattak, M. Ul-Islam, M. W. Ullah, B. Yu, S. Khan and J. K. Park, *Process Biochem.*, **49**, 357 (2014).
13. J. H. Ha, N. Shah, M. Ul-Islam and J. K. Park, *Enzyme Microb. Technol.*, **49**, 298 (2011).
14. J. H. Ha, M. K. Gang, T. Khan and J. K. Park, *Korean J. Chem. Eng.*, **29**, 1224 (2012).
15. W. A. Khattak, M. Kang, M. Ul-Islam and J. K. Park, *Bioproc. Biosyst. Eng.*, **36**, 737 (2013).
16. V. V. Kushnirov, *Yeast*, **16**, 857 (2000).

17. A. Conzelmann, H. Riezman, C. Desponds and C. Bron, *EMBO J.*, **7**, 2233 (1988).
18. A. Horwath and H. Riezman, *Yeast*, **10**, 1305 (1994).
19. H. Riezman, T. Hase, V. L. Apgm, L. A. Grivell, K. Suda and G. Schatz, *EMBO J.*, **2**, 2161 (1983).
20. W. A. Khattak, M. Ul-Islam and J. K. Park, *Korean J. Chem. Eng.*, **29**, 1467 (2012).
21. A. Tilman and D. H. Wolf, *Yeast,* **1**, 139 (1985).
22. J. M. Berg, J. L. Tymoczko and L. Stryer, *Biochemistry, 5th Ed.*, W. H. Freeman, New York (2002).
23. E. M. Algar and R. K. Scopes, *J. Biotechnol.*, **2**, 275 (1985).
24. K. Blinova, S. Carroll, S. Bose, A. V. Smirnov, J. J. Harvey and J. R. Knutson, *Biochemistry*, **44**, 2585 (2005).
25. M. L. Shuler and F. Kargi, *Bioprocess Engineering: Basic concepts*, Prentice Hall, New Jersey (2001).
26. J. Postmus, A. B. Canelas, J. Bouwman, B. M. Bakker, W.-V. Gulik and M. J. de Mattos, *J. Biol. Chem.*, **283**, 23524 (2008).
27. A. L. B. Cruz, M. Hebly, G. H. Duong, S. A. Wahl, J. T. Pronk and J. J. Heijnen, *BMC Syst. Biol.*, **6**, 151 (2012).
28. D. U. Silverthorn, *Human Physiology: An Integrated Approach*, Addison-Wesley, Boston (2004).
29. S. C. Kwon, S. J. Park, J. M. Cho, *J. Ind. Microbiol.*, **17**, 30 (1996).
30. H. Rikimaru, N. Stanford and W. H. Stein, *J. Biol. Chem.*, **248**, 2296 (1973).
31. C. Ching-san, Y. Tsong-rong and C. Her-yuan, *J. Food Biochem.*, **2**, 349 (1978).
32. A. Dong, B. Caughey, W. S. Caughey, K. S. Bhat and J. E. Coe, *Biochemistry*, **31**, 9364 (1992).
33. H. Susi and D. M. Byler, *Methods Enzymol.*, **130**, 290 (1986).
34. D. M. Byler and H. Susi, *Biopolymer.*, **25**, 469 (1986).
35. P. I. Haris and F. Severcan, *J. Mol. Catal. B: Enzym.*, **7**, 207 (1999).
36. A. Elliott and E. J. Ambrose, *Nature*, **165**, 921 (1950).
37. S. Krimm and J. Bandekar, *Adv. Protein Chem.*, **38**, 181 (1986).
38. J. Banker, *Biochim. Biophys. Acta*, **1120**, 23 (1992).
39. T. Miyazawa, *J. Chem. Phys.*, **32**, 1647 (1960).
40. Y. G. Jin, W. W. Fu and M. H. Ma, *Afr. J. Biotechnol.*, **10**, 10204 (2011).
41. W. H. Wang, X. P. Li and X. Q. Zhang, *Pigm. Resin. Technol.*, **37**, 93 (2008).
42. J. Kong and S. Yu, *Acta. Bioch. Bioph. Sin.*, **39**, 549 (2007).
43. M. M. M. Wilhelmus, R. M. W. de Waal and M. M. Verbeek, *J. Mol. Neurobiol.*, **35**, 203 (2007).
44. M. E. Gómez, J. M. Igartuburu, E. Pando, F. R. Luis and G. Mourente, *J. Agr. Food Chem.*, **52**, 4791 (2004).

Supporting Information

Enhanced bio-ethanol production via simultaneous saccharification and fermentation through a cell free enzyme system prepared by disintegration of waste of beer fermentation broth

Shaukat Khan, Mazhar Ul-Islam, Waleed Ahmad Khattak, Muhammad Wajid Ullah, Bowan Yu, and Joong Kon Park†

Department of Chemical Engineering, Kyungpook National University, Daegu 702-701, Korea
(*Received 27 March 2014 • accepted 21 August 2014*)

Table 1S. Disintegrated sediment (20%) analyzed by LC–MS/MS (Q-TOF) using the mascot algorithm to identify yeast cellular proteins

Class	Accession No.	Description	Taxonomy	Mass (Da)	PI	Score
Glycolytic	gi|14318578	Hexokinase 1p	*S. cerevisiae*	53933	5.28	2182
	gi|6319673	Phosphoglucose isomerase 1p	*S. cerevisiae*	61261	6	2408
	gi|6322790	Aldolase	*S. cerevisiae*	39881	5.51	136
	gi|230405	Triphospahate isomerase	*S. cerevisiae*	26762	5.75	3689
	gi|6324951	Glyceraldehydes Phosphate dehydrogenase	*S. cerevisiae*	49881	5.56	867
	gi|10383781	Phosphoglycerate kinase	*S. cerevisiae*	44768	7.11	40
	gi|223471	Phosphoglycerate mutase	*S. cerevisiae*	26900	9.05	59
	gi|171455	Enolase	*S. cerevisiae*	46830	6.16	2011
	gi|4180	Pyruvate kinase	*S. cerevisiae*	54964	8	48
Fermentation	gi|6323073	Pyruvate decarboxylase	*S. cerevisiae*	61685	5.8	633
	gi|6324486	Alcohol dehydrogenase	*S. cerevisiae*	37282	6.21	3872
Protease	gi|398365031	Carboxypeptidase ysc Y	*S. cerevisiae*	58229	7.2	33
	gi|3368	Aminopeptidase ysc II	*S. cerevisiae*	97646	6.03	414

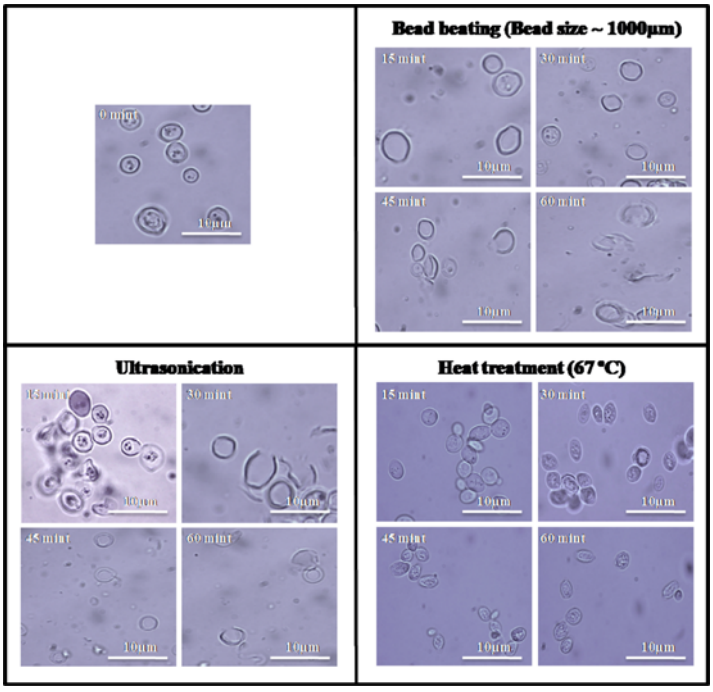

Fig. 1S. Cell morphology by fluorescent microscopy after various time intervals during disintegration by the indicated methods. Cells contained in the WBFB were treated by different cell lysis methods.